

Evolution of temperature, O₃, CO, and N₂O profiles during the exceptional 2009 Arctic major stratospheric warming as observed by lidar and millimeter-wave spectroscopy at Thule (76.5°N, 68.8°W), Greenland

Claudia Di Biagio,^{1,2} Giovanni Muscari,³ Alcide di Sarra,¹ Robert L. de Zafra,⁴
Paul Eriksen,⁵ Giorgio Fiocco,⁶ Irene Fiorucci,³ and Daniele Fuà⁶

Received 18 February 2010; revised 10 September 2010; accepted 22 September 2010; published 31 December 2010.

[1] The 2009 Arctic sudden stratospheric warming (SSW) was the most intense event of this kind ever observed. Unique ground-based measurements of middle atmospheric profiles for temperature, O₃, CO, and N₂O obtained at Thule (76.5°N, 68.8°W), Greenland, in the period January to early March are used to show the evolution of the 2009 SSW in the region of its maximum intensity. The first sign of the SSW was detected at $\theta \sim 2000$ K on 19 January, when a rapid decrease in CO mixing ratio took place. The first evidence of a temperature increase was observed at the same level on 22 January, the earliest date on which lidar measurements reached above ~50 km. The warming propagated from the upper to the lower stratosphere in 7 days and the record maximum temperature of 289 K was observed between 1300 and 1500 K potential temperature on 22 January. A strong vortex splitting was associated with the SSW. Stratospheric backward trajectories indicate that air masses arriving at Thule during the warming peak underwent a rapid compression and an intense adiabatic warming of up to 50 K. The rapid advection of air from the extratropics was also occasionally observed to produce elevated values of N₂O mixing ratio. Starting in mid-February the temperature profile and the N₂O mixing ratio returned to the prewarming values in the mid and upper stratosphere, indicating the reformation of the vortex at these levels. In late winter, vertical descent from starting altitudes of ~60 km is estimated from CO profiles to be 0.25 ± 0.05 km/day.

Citation: Di Biagio, C., G. Muscari, A. di Sarra, R. L. de Zafra, P. Eriksen, G. Fiocco, I. Fiorucci, and D. Fuà (2010), Evolution of temperature, O₃, CO, and N₂O profiles during the exceptional 2009 Arctic major stratospheric warming as observed by lidar and millimeter-wave spectroscopy at Thule (76.5°N, 68.8°W), Greenland, *J. Geophys. Res.*, 115, D24315, doi:10.1029/2010JD014070.

1. Introduction

[2] Sudden stratospheric warmings (SSWs) are the most important perturbing events that affect the dynamics and thermal structure of the winter stratosphere in the Northern Hemisphere. The 2008–2009 Arctic winter has been characterized as the largest major SSW event ever observed [Labitzke and Kunze, 2009; Manney *et al.*, 2009; Harada *et al.*, 2010]. The development of SSWs is linked to the vertical propagation of planetary waves, which dissipate first in the mesosphere and then progressively through the

stratosphere, interacting with the westerly winter circulation and modifying the atmospheric thermal profile from the upper troposphere through the mesosphere [Schoeberl, 1978]. Major warmings produce the breakdown of the winter circulation through either the displacement or the splitting of the polar vortex, the instauration of an easterly circulation, and the reversal of the latitudinal temperature gradient. Strong differences in terms of dynamics, transport, and evolution of the stratospheric chemical composition and of the vertical structure of the polar vortex exist between displacement and splitting events [Charlton and Polvani, 2007; Manney *et al.*, 2009; Mathewman *et al.*, 2009]. Minor events are less intense and do not produce the reversal of the mean zonal circulation.

[3] The Arctic stratosphere is characterized by large interannual variability, and very warm winters can alternate with cold ones. The occurrence of SSWs has been shown to be connected to the phase of the quasi-biennial oscillation, to the solar cycle [Labitzke and van Loon, 1988], and to the Southern Oscillation [van Loon and Labitzke, 1987].

¹ENEA/UTMEA-TER, Rome, Italy.

²Also at Department of Earth Science, University of Siena, Siena, Italy.

³Istituto Nazionale di Geofisica e Vulcanologia, Rome, Italy.

⁴Department of Physics and Astronomy, State University of New York at Stony Brook, Stony Brook, New York, USA.

⁵Danish Meteorological Institute, Copenhagen, Denmark.

⁶Department of Physics, “Sapienza” University of Rome, Rome, Italy.

As discussed by *Charlton and Polvani* [2007], frequent sudden warmings occurred in the period 1958–2002, with a mean of six major events per decade observed. Series of minor warmings or single minor events typically alternate with major SSWs [*Schoeberl*, 1978; *Manney et al.*, 2005].

[4] An increasing number of large warming events has been registered during the last 10 years [*Manney et al.*, 2005]. Before the winter of 2008–2009, the most intense recent warmings in the Arctic were detected in 2004 and 2006 [*Manney et al.*, 2005, 2008].

[5] The 2009 SSW described here using ground-based observations started in mid-January and was accompanied by an intensification of planetary wave 2. As the SSW developed the stratopause lowered and the mean zonal circulation reversed, proceeding from the mesosphere downward. Studies by *Manney et al.* [2009] (using satellite-based measurements), by *Labitzke and Kunze* [2009] (using the European Centre for Medium-Range Weather Forecast (ECMWF) reanalyses), and by *Harada et al.* [2010] (using the Japan Meteorological Agency reanalyses) describe the mean evolution of the warming event over the entire Arctic region, thus providing a global view of the 2009 winter. The reversal of the 10 hPa zonal mean zonal wind at 60°N occurred on about 22 January [*Manney et al.*, 2009]. As the SSW propagated downward it induced a splitting of the polar vortex in the lower stratosphere. The maximum warming, at 10 hPa, took place on 24 January above Greenland due to the dominant planetary wave 2 [*Labitzke and Kunze*, 2009] during the SSW. At the end of January the stratopause disappeared and a quasi-isothermal stratospheric temperature profile was observed. A strong polar vortex re-formed very rapidly in the upper stratosphere in the beginning of February. The 10 hPa, 60°N westerly circulation was restored in the beginning of March.

[6] In the present study, ground-based observations of the thermal structure and chemical composition of the middle atmosphere from the Network for Detection of Atmospheric Composition Change (NDACC; <http://www.ndsc.ncep.noaa.gov/>) station at Thule Air Base (76.5°N, 68.8°W), Greenland, are used to show the evolution of the phenomenon and its interactions with the dynamical structure of the polar vortex in the region of maximum warming [*Labitzke and Kunze*, 2009].

2. Measurements

[7] An intensive measurement campaign was conducted in Thule during January to early March 2009, with a lidar (“Sapienza” University of Rome) and a ground-based millimeter-wave spectrometer (GBMS; Stony Brook University, Stony Brook, New York). The lidar was installed at Thule in 1990 and has been operational for several years, particularly during the winter season [e.g., *di Sarra et al.*, 2002, and references therein; *Keckhut et al.*, 2004]. The transmitter of the lidar system is composed of a two-stage Nd:YAG laser, with a second harmonic generator producing linearly polarized pulses of a nominal energy of ~200 mJ at 532 nm, at a repetition rate of 10 Hz. The divergence of the laser beam is less than 1 mrad. The receiver includes an 0.8 m diameter Cassegrain telescope and a photon counting acquisition system. The parallel and cross-polarized components of the backscattered signal are separately acquired.

A chopper is used to cut off signals from the lowest atmospheric levels, to prevent the saturation of the photomultiplier tubes. Atmospheric temperature (T) profiles were derived from 25 up to 70 km altitude by applying the algorithm described by *Marenco et al.* [1997]. T was derived with a vertical resolution of 150 m and averaged over 4.5 km. To reduce the signal-to-noise ratio the signal was integrated for 1–5 h, depending on the weather conditions. The estimated 1σ uncertainty varies from ~1 K at 25 km to ~15 K at the maximum probed altitude. National Centers for Environmental Predictions (NCEP) reanalyses over Thule and radiosonde data obtained from the stations at Eureka (79.9°N, 85.9°W) and Alert (82.5°N, 62.3°W) were used to provide temperatures below 25 km.

[8] The GBMS has been operated most recently prior to 2009 at Thule during the winters of 2001–2002 and 2002–2003 [*Muscati et al.*, 2007, and references therein]. The GBMS measures rotational emission spectra of atmospheric chemical species such as O₃, N₂O, CO, and HNO₃, as well as the H₂O continuum, with a spectral window of 600 MHz tunable between approximately 230 and 280 GHz. It comprises a front-end receiver employing a cryogenically cooled SIS mixer and a back end composed of an acousto-optical spectrometer [*de Zafra*, 1995]. By means of the observed line shape together with pressure and temperature vertical profiles, a mathematical deconvolution process allows finding the emitting molecule’s concentration as a function of altitude from about 15 to 80 km. For water vapor, only the integrated column contents can be obtained [*Fiorucci et al.*, 2008]. O₃ and CO spectra are measured with an ~1.5 h integration, while HNO₃ and N₂O lines are weaker and need about 3–4 h of integration. The vertical resolution of the GBMS is limited by the inversion algorithm and averages one pressure scale height: the nominal vertical resolution is 6–8 km, although relative peaks in concentration profiles can be determined within ±1 km altitude. Detailed information on the observing technique and GBMS data analysis is given by *de Zafra* [1995] and *Muscati et al.* [2007].

[9] The GBMS retrieval algorithm has recently changed to a standard optimal estimation method (OEM), which was applied to the O₃ and N₂O measurements reported here. Careful comparisons of mixing ratio (mr) profiles obtained with previous [*Muscati et al.*, 2007, and references therein] and current algorithms show no significant differences in results and error estimates, with the OEM providing, however, additional information needed to better characterize the retrievals and compare them to other data sets. Further refinements of and validation efforts on O₃ and N₂O OEM retrievals are still under way, and results reported here should be considered preliminary. CO retrievals, instead, have not yet undergone such testing, and vertical profiles reported in this article are therefore still obtained using the Chahine-Twomey method [*de Zafra and Muscati*, 2004, and references therein]. O₃, N₂O, and CO measurements have an estimated 1σ uncertainty of 13% (minimum, 0.3 ppmv), 15% (minimum, 5 ppbv), and 16% (minimum, 0.1 ppmv), respectively.

[10] During January to early March 2009, lidar and GBMS measurements were usually performed on a daily basis, except during periods characterized by poor weather

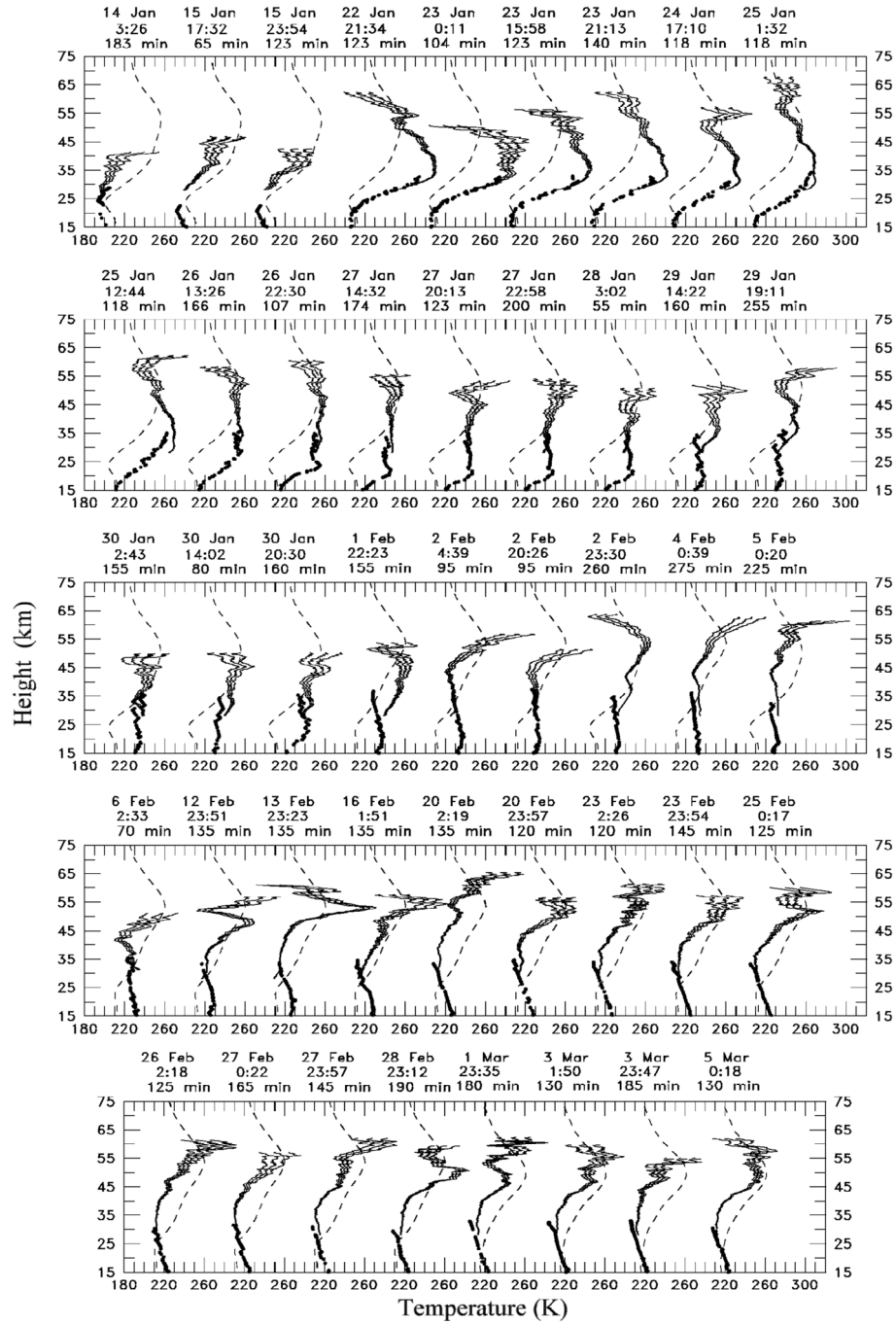


Figure 1. Lidar temperature profiles obtained between 14 January and 5 March 2009 at Thule. T , $T + \sigma$, and $T - \sigma$ are shown. The dashed line represents the CIRA 1986 model [Barnett and Corney, 1985] for the month. Dotted profiles are radiosonde data that are the closest in time data (from Eureka or Alert, depending on the data availability). Date, time, and integration time in minutes are reported.

conditions (both instruments, 5–11 February) or instrument malfunctioning (lidar, 16–22 January).

3. Results and Discussion

3.1. Temporal Evolution of the Middle Atmosphere Thermal Structure

[11] Figure 1 shows the temporal evolution of temperature profiles measured by lidar between 14 January and 5 March

2009 at Thule. The maximum altitude in the derived temperature depends on the time of integration, presence of clouds, and background noise. Initial profiles reached only up to 45–50 km. The agreement between lidar temperature profiles and radiosonde data is generally good (see overlapped profiles in Figure 1), despite the distance of more than 400 km between Thule and both Eureka and Alert.

[12] In mid-January, before the SSW event, a cold vortex was stably present (see Figure 1, profiles of 14 and 15 January,

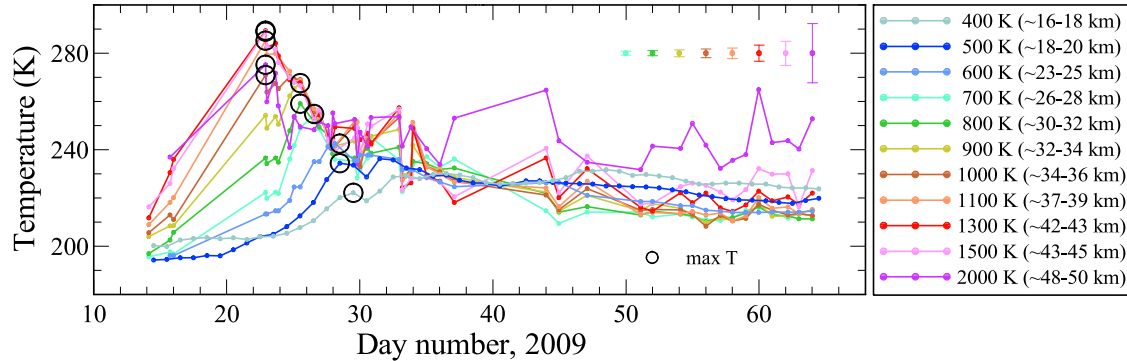


Figure 2. Temporal evolution of stratospheric temperature interpolated at different θ levels between 400 and 2000 K (temperatures at 400, 500, and 600 K are from National Centers for Environmental Predictions (NCEP) reanalyses) in the period 14 January to 5 March 2009 (days 14–64). Maximum 1σ uncertainties at the different levels are indicated by vertical bars. Maximum temperature obtained at each level due to downward propagation of the warming is highlighted by a circle.

and Figure 7, maps of 17 January). An ozone sonde launched from Thule on 12 January showed that conditions for polar stratospheric cloud (PSC) formation were already present on that date at an altitude of about 19 km. Type Ia PSC particles were detected by lidar on January 17 and 18 between 17 and 22 km (not shown).

[13] Starting on 22 January, a sudden increase in the temperature profiles was observed in the region below about 50 km. Because initial lidar profiles reached only up to ~50 km, and because of the lack of measurements between 15 and 22 January, the first thermal measure of warming was observed on 22 January, although we show here that a dramatic change in high-altitude CO was seen to begin on 19 January.

[14] Temperatures higher than 280 K were measured on January 22 between about 31 and 43 km altitude. On January 24 at the altitude of 30 km (~10 hPa), the temperature was 273 K, consistent with the warming peak values reported over Thule by Labitzke and Kunze [2009] in their Figure 4. The temperature profile became nearly isothermal over the wide vertical range 24–55 km at the end of January (days 27–28, $T \sim 240$ K) and then between approximately 15 and 45 km altitude at the beginning of

February (days 35–37, $T \sim 230$ K). From mid-February (days 43–44) to the beginning of March, the temperature profile returned to the prewarming values above 35 km altitude, owing to the restoration of the polar vortex (see Figure 5), while it remained up to 30 K warmer than in the prewarming period at lower levels, where the vortex never re-formed during the time monitored here.

[15] On January 22 the stratopause (identified as the height of the maximum stratospheric temperature) was observed at about 35 km altitude. It descended to about 30 km on 25 January. With the development of the isothermal profile noted in the preceding paragraph, a local maximum appeared at about 25 km on 26 January, progressively descending to 20 km on 29 January. In early February a T maximum appeared near 52 km and remained between 45 and 55 km until early March.

[16] Figure 2 shows the temporal evolution of T at different potential temperature (θ) levels between 400 and 2000 K (~16 to 50 km) during the period 14 January to 5 March 2009 (days 14–64). The highest temperatures occurred on 22 January at the highest sounded levels. The warming reached 800–1000 K after 2–4 days (24–26 January) and 400–600 K after 6–7 days (28–29 January). The value of

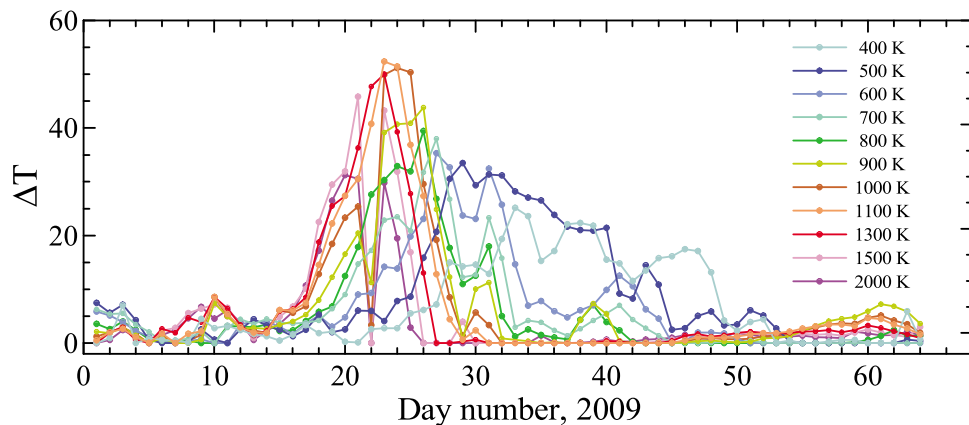


Figure 3. Temporal evolution of the temperature difference (ΔT) between the air-mass final T over Thule and the minimum T reached by the air parcel along 5 day isentropic backward air-mass trajectories for θ levels between 400 and 2000 K in the period 1 January to 5 March 2009 (days 1–64).

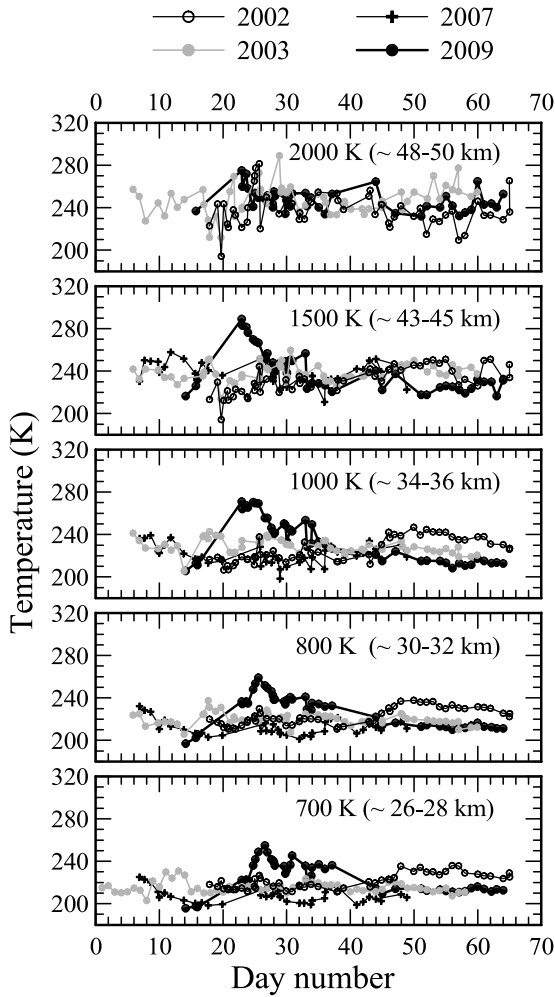


Figure 4. Temporal evolution of the temperature measured by lidar at various θ levels between 700 and 2000 K for the winters of 2002, 2003, 2007, and 2009, all characterized by major warming events.

the maximum T reached at each level owing to the downward propagation of the warming decreased approximately linearly with θ , from 289 K at layers between 1300 and 1500 K (22 January) to 222 K at level 400 K (30 January).

[17] To relate the warming event to the dynamical situation, we calculated temperature variations along 5 day isentropic backward air-mass trajectories arriving at Thule. Trajectories were obtained from the NASA Goddard Space Flight Center (GSFC) Automailer system [Schoeberl and Sparling, 1994] using NCEP reanalysis data. One trajectory per day ending at Thule at 0000 UT was used in the analysis. The difference ΔT between the air-mass final temperature over Thule and the minimum T reached by the air parcel during its 5 day run is indicative of the adiabatic heating taking place along the trajectory. Figure 3 shows the temporal evolution of ΔT for θ levels between 400 and 2000 K in the period 1 January to 5 March (days 1–64). ΔT is always <10 K at all levels, except when the warming occurs. ΔT for the days of maximum warming is ~ 50 K at 1000 \div 1300 K and between 25 and 45 K at the other selected θ levels. The corresponding air-mass compression

Δp , measured as the difference between the air parcel final pressure over Thule and the minimum pressure reached along its 5 day isentropic trajectory, is estimated to produce a 30%–50% pressure increment. The compression occurs later at the lowest levels, consistently with the evolution of the warming. Thus, air parcels on the trajectories approaching the polar region during the warming peak were subjected to a rapid compression and an intense adiabatic heating that largely contributed to the total observed warming.

3.2. Previous Sudden Stratospheric Warnings Measured at Thule by Lidar

[18] Figure 4 shows the temporal evolution of the temperatures measured by lidar at θ levels between 700 and 2000 K for the winters of 2002, 2003, 2007, and 2009, all affected by major warmings. It should be pointed out that the two previously most intense SSWs of the decade were those of 2004 and 2006 [Manney et al., 2005, 2008]; no lidar measurements were carried out at Thule during these two winters, so we cannot directly relate the 2009 SSW with the warmings of 2004 and 2006. However, Manney et al. [2009] have already compared the three events and have shown that the 2009 warming was more intense than those of 2004 and 2006, producing stronger and more prolonged effects on the lower stratospheric dynamics and structure.

[19] The 2009 SSW was characterized by the highest absolute temperatures and by the largest temperature gradient versus time ever observed at Thule by lidar. The maximum temperature of 289 K at 42–45 km (potential temperature levels between 1300 and 1500 K) is up to 40 K higher than maxima observed during the winters of 2002, 2003, and 2007, and the T gradient peaked at 42 km, with ~ 9 K/day, between 14 and 22 January. Temperatures between 35 and 45 km altitude (1000–1500 K potential temperature levels) were consistently lower throughout February and early March than in the other winters considered here.

3.3. Chemical Composition and Vortex Evolution

[20] Figure 5 shows the temporal evolution of Ertel's potential vorticity (PV), T , N_2O , CO, and O_3 mr's above Thule, at different θ levels between 500 (~ 18 –20 km) and 2000 K (~ 48 –50 km), in the period 14 January to 5 March 2009. The PV values were obtained from the NASA GSFC Automailer system, based on NCEP data. Estimates of PV values corresponding to the inner vortex edge during January are also given in Figure 5. Figure 6 shows polar plots obtained using Aura/Microwave Limb Sounder (MLS) measurements from 13 January 2009, downloaded from <http://mls.jpl.nasa.gov/data/gallery.php> (courtesy of Gloria Manney). They are used here to show the overall chemical and dynamical status of the Arctic region before the SSW. Approximate values of N_2O and CO at the various potential temperature levels can be read on the corresponding scales and are consistent with GBMS values reported in Figure 5. Figure 6 shows that extravortex stratospheric air is richer in N_2O and poorer in CO with respect to in-vortex air. Upper stratospheric Aura/MLS maps for O_3 are useful to show that a combination of photochemistry and dynamics causes large O_3 gradients between the vortex edge and its inner region (characterized by little sun exposure and low O_3 mr's).

[21] PV values in Figure 5 show that the splitting of the vortex, concurrent with the passage of the vortex edge above

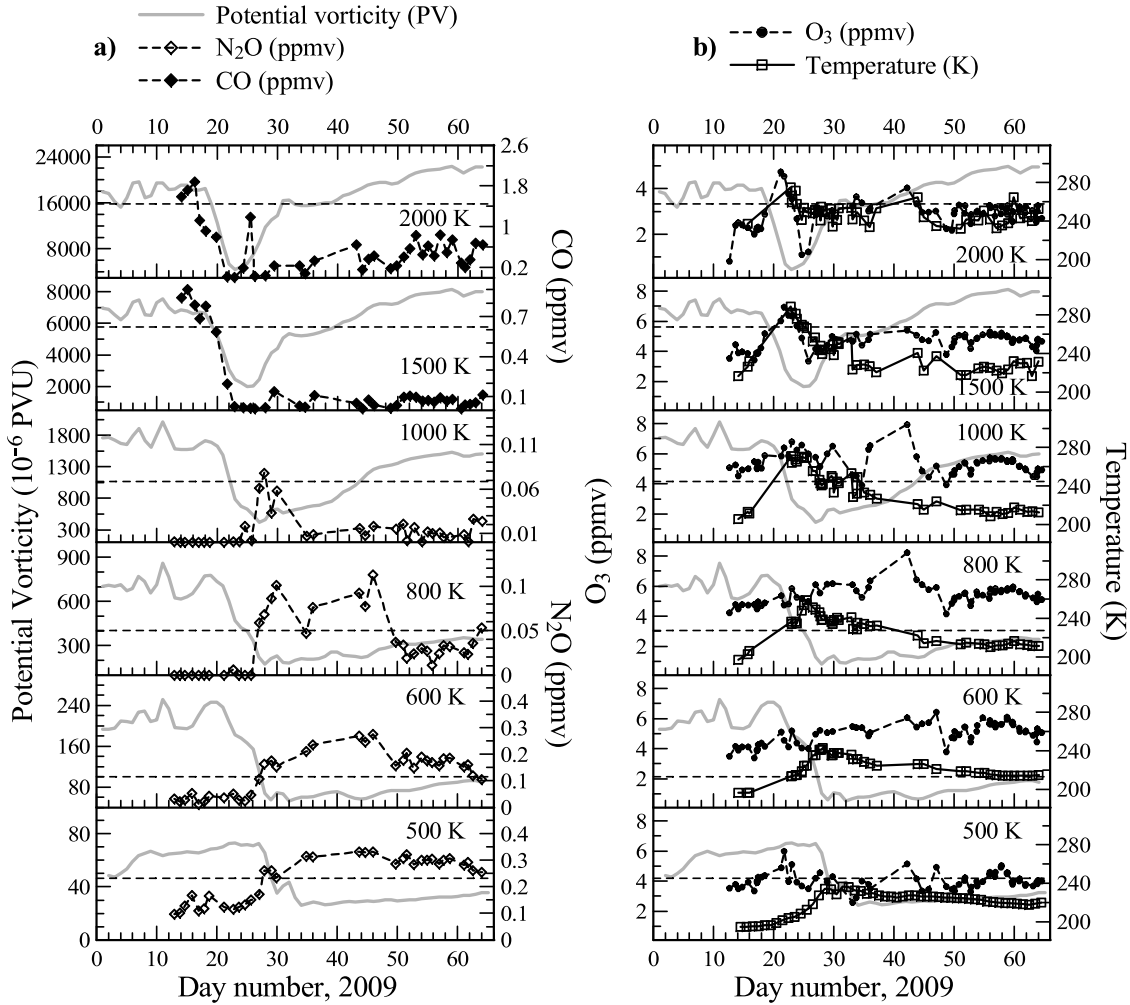


Figure 5. Temporal evolution of (a) Ertel's potential vorticity (PV; 1 PV unit (PVU) = $1 \text{ K m}^2 \text{ kg}^{-1} \text{ s}^{-1}$), N_2O , and CO mixing ratio (mr); (b) O_3 mr and temperature, at θ levels between 500 and 2000 K in the period 14 January to 5 March 2009 (days 14–64). Temperatures at 500 and 600 K are from NCEP reanalyses. Horizontal dashed lines are indicative threshold values for the inner vortex edge.

Thule, progressed from the top downward and took about 8 days to reach the lower stratosphere (about 20 January at 2000 K and 28 January at 500 K). Figure 7 shows Northern Hemisphere PV maps (obtained from ECMWF reanalysis data) at the potential temperature levels of 950 and 550 K for selected days between 17 and 30 January. At 950 K the vortex was stably present above Thule until 22–23 January, when the splitting occurred at this level and the transition from inside to outside the vortex caused the rapid decrease in PV. This transition was not observed at Thule until 27 January at 550 K. These results are in agreement with our analyses at 1000 K and 500–600 K, respectively, based on PV data shown in Figure 5.

[22] As is apparent in Figure 5, between 1000 and 500 K the passage of the vortex edge over Thule associated with the vortex breakup was accompanied by a sudden increase in N_2O mr that occurred between 26 and 28 January. The observed increase brought N_2O mr values of about 0.25, 0.15, 0.10, and 0.08 ppmv at 500, 600, 800, and 1000 K, respectively, values representative of low- to mid-latitude air (see also Figure 6). At all these levels PV and N_2O are in

good agreement regarding identification of the vortex breakup (decreasing PV, increasing N_2O), although the exact timing might be slightly off, depending on the PV value chosen as indicative of the vortex inner edge. Figure 8 shows isentropic 10 day backward air-mass trajectories obtained from the NASA GSFC Automailer system for the levels 500, 800, and 1500 K ending at Thule at 0000 UT on 17, 23, and 30 January, 15 February, and 1 March 2009. At 500 K and 800 K, until the end of January, when the vortex breakup occurred, air-mass trajectories indicate the presence of a typical vortex circulation (trajectories for 17 and 23 January); from the end of January, air masses from mid and low latitudes were advected over Thule (see, e.g., the trajectory for 30 January at 800 K), thus explaining the rapid increase in N_2O mr immediately after the vortex breakup.

[23] At higher levels, because of the rapid vertical decrease in both the nitrous oxide mr and its gradient across the vortex edge, N_2O becomes less reliable in describing the origin of the observed air masses. Instead, CO becomes a better tool for this purpose [e.g., de Zafra and Muscari, 2004]. At these levels the vortex splitting and the vortex

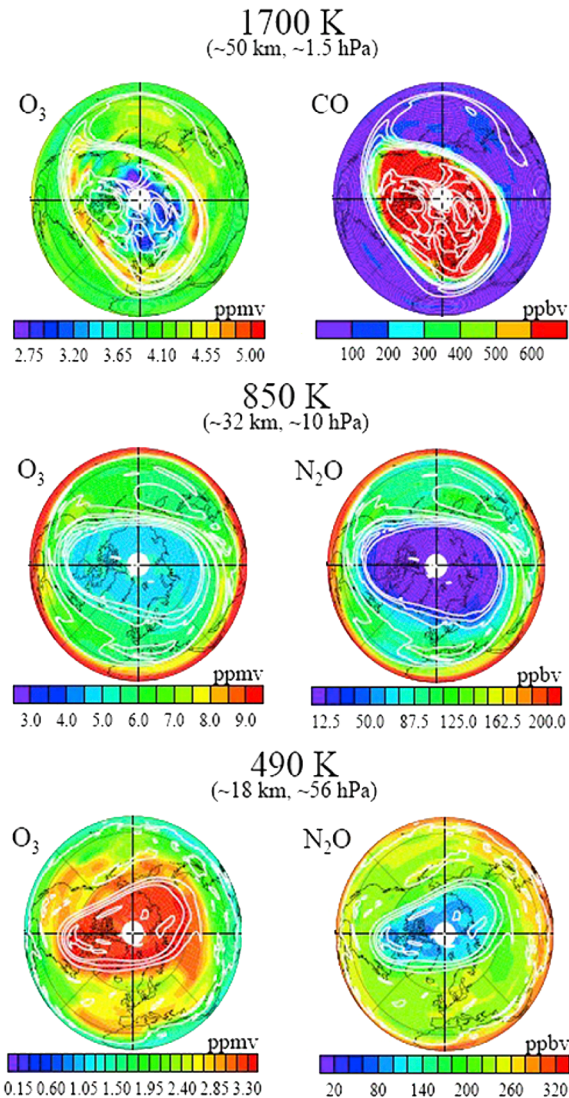


Figure 6. Contour plots of Aura/Microwave Limb Sounder (MLS) O_3 , N_2O , and CO mr's at three potential temperature levels on 13 January 2009 (courtesy of Gloria Manney and the MLS Team). White contours are typically scaled PV values from GEOS-5. For additional plots and information, see <http://mls.jpl.nasa.gov/data/gallery.php>.

edge transit over Thule were marked by a rapid decrease in CO mr matching the PV decrease. CO data in Figure 5 indicate that at 2000 and 1500 K, the vortex broke up over Thule on 19–20 January. GBMS CO mr variations during the warming were observed to be about -0.2 and -0.35 ppmv/day at 1500 and 2000 K, respectively.

[24] Concurrently, as warm, O_3 -rich air from outside the vortex moved over Thule during the SSW, the GBMS measured an increase in O_3 mr in the upper stratosphere of 0.8 and 0.6 ppmv/day at 1500 and 2000 K, respectively. Air masses coming from low and mid latitudes were advected over Thule at 1500 K in the same period (see the trajectories for 23 and 30 January in Figure 8).

[25] On late 25 January, shortly after the vortex breakup, a decrease in O_3 mr (about 3.6 ppmv) concurrent with a

rapid and strong increase in CO mr (about 1.2 ppmv) between 1700 and 2000 K (only level 2000 K is shown in Figure 5) suggests that a parcel originating from the former inner vortex was advected over Thule at these levels (see also the O_3 and CO distribution in the inner vortex region from the AURA/MLS maps in Figure 6). This parcel of vortex air above Thule is not present in the PV reanalysis data. This indicates that GBMS tracer measurements may identify air parcels more accurately than PV reanalyses, which have an inherent coarser temporal and spatial resolution.

[26] After such an intense SSW, air parcels in the newly formed vortex can be characterized by very different chemical tracer contents. The history of air masses contained in this re-formed vortex is therefore defined by their tracer concentrations (which are related to chemical and dynamics processes) more accurately than by their position inside the vortex (i.e., PV values, which are due to the radiative cooling in the polar night region), and a strict consistency between chemical tracer mr and PV values should not be expected. During February, PV values indicate that the vortex re-formed rapidly and strongly at higher levels (between about 6 and 12 February at 2000, 1500, and 1000 K) but not in the lower stratosphere (below about 800 K). Figure 8 shows that a stable winter circulation, with air masses confined inside the polar vortex, was restored at the 1500 K level starting in the second half of February.

[27] At 500 K stable conditions with no vortex reformation were maintained until early March and the observed N_2O mr remained almost constant (about 0.3 ppmv) from the beginning of the SSW event, thus indicating well-mixed extravortex air masses. This is in agreement with back-trajectory analyses indicating the advection of air masses originating from mid and high latitudes over Thule (see Figure 8). At 800 K the N_2O mr shows more variability with respect to level 500 K, with higher values from immediately after the warming event (day 27) through mid-February, indicating extravortex air masses, and lower values from day 50 to the end of the campaign, indicating the observation of vortex air. Figure 8 shows air masses from North Africa arriving over Thule on 30 January and on 15 February, therefore explaining the increase and the two relative maxima of the N_2O mr at 800 K (~ 0.11 ppmv) observed on these two days. Additional Aura/MLS contour maps at 850 K (<http://mls.jpl.nasa.gov/data/gallery.php>) show the complex structures of filaments of both residual and new vortex air formed during February and early March above the entire Arctic area, and the presence of these filaments may in part explain the observed N_2O and O_3 variability. At 1000 K, after the SSW event, the N_2O mr rapidly returns to low values, indicating the rapid reformation of a strong vortex with somewhat mixed vortex and mid-latitude air inside.

[28] CO mr values at 1000 K and above 2000 K (data not shown) suggest the same scenario, with a rapid return to higher values shortly after the SSW and some variability due to vortex and extravortex filaments (e.g., a sudden drop on day 42 at 1000 K, matching in time the large O_3 mr peak shown in Figure 5). In the extended altitude range from 1300 to 2000 K, however, CO does not show the same significant increase in mr from early February onward (see Figure 5), and the GBMS must be sampling extravortex air inside the re-formed vortex, as discussed previously. Figure 9 shows a contour plot of CO mr between 45 and 70 km in the period

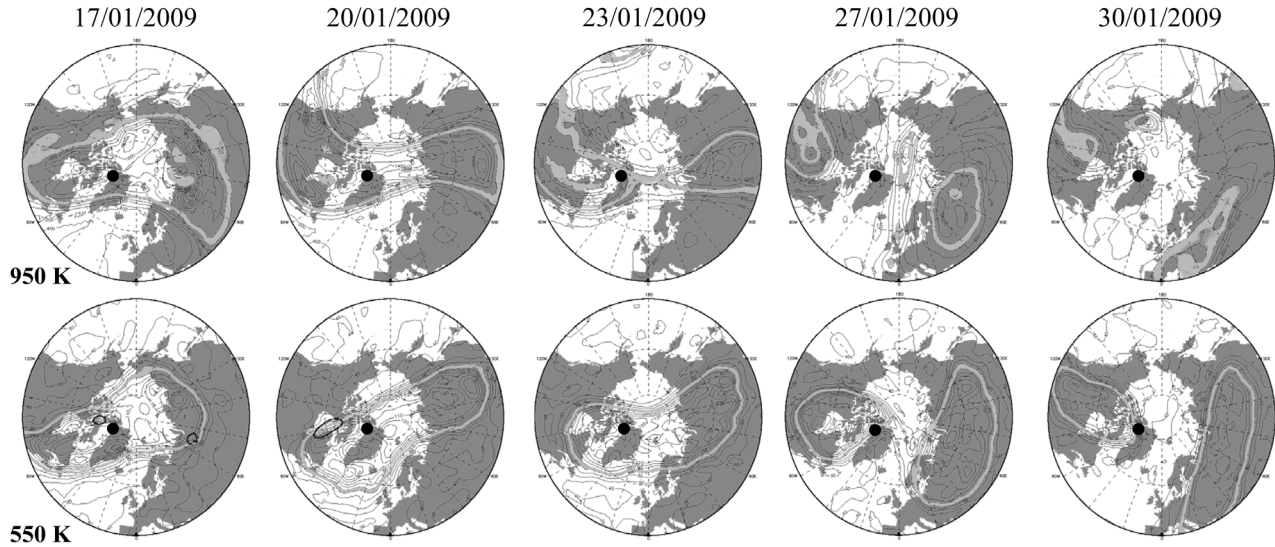


Figure 7. Northern Hemisphere PV maps (obtained from European Centre for Medium-Range Weather Forecast reanalysis data) at potential temperature levels of 950 K (top) and 550 K (bottom) for 17, 20, 23, 27, and 30 January 2009. Light gray lines correspond to the inner vortex edge; black lines indicate the threshold temperatures for the formation of polar stratospheric clouds at the two levels. The position of Thule is indicated by filled circles.

14 January to 5 March (days 14–64). From mid-February to early March, GBMS CO observations followed the vertical descent of air inside the reestablished polar vortex that results from the return flow of the meridional residual circulation. Seven CO mr levels, from 5 to 11 ppmv, were followed as they descended with time inside the vortex,

and three of these linear regressions (for 5, 8, and 11 ppmv) are indicated in Figure 9 by bold dashed lines. In mid-February the indicated range of CO mr values encompasses descent starting altitudes between 58 and 62 km. The seven linear regressions (all characterized by a squared correlation coefficient >0.83) indicate descent rates of from 0.20 ± 0.05

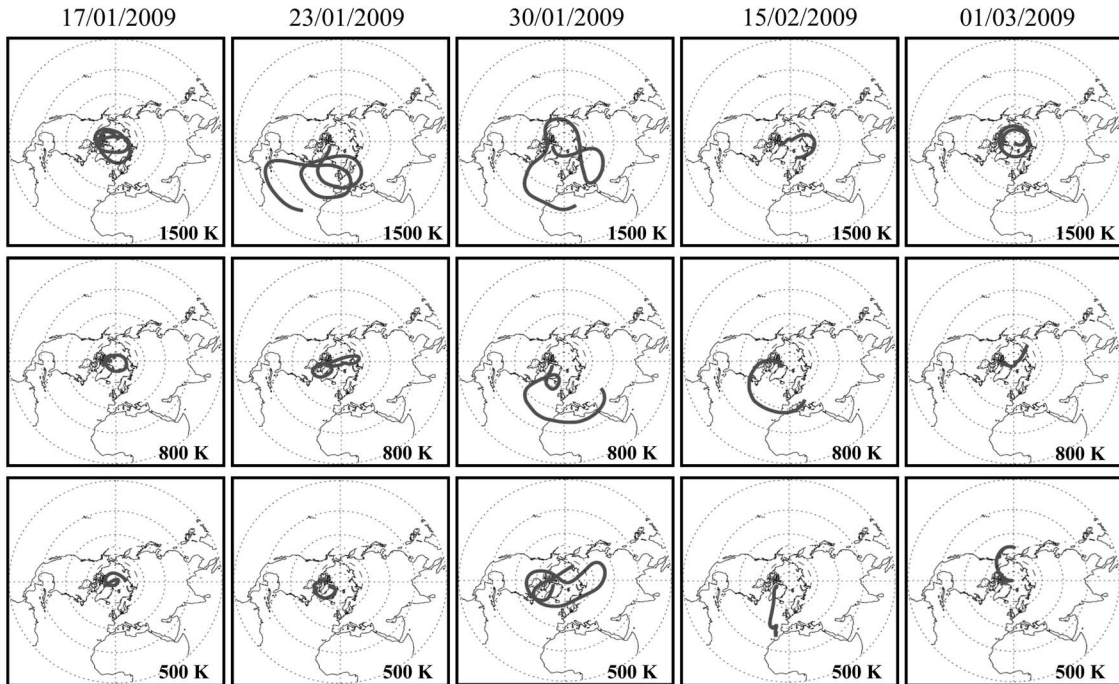


Figure 8. Isentropic 10 day backward air-mass trajectories for the levels 500, 800, and 1500 K ending at Thule at 0000 UT on 17, 23, and 30 January, 15 February, and 1 March 2009. Trajectories were obtained from the NASA Goddard Space Flight Center Automailer system [Schoeberl and Sparling, 1994] using NCEP reanalysis data.

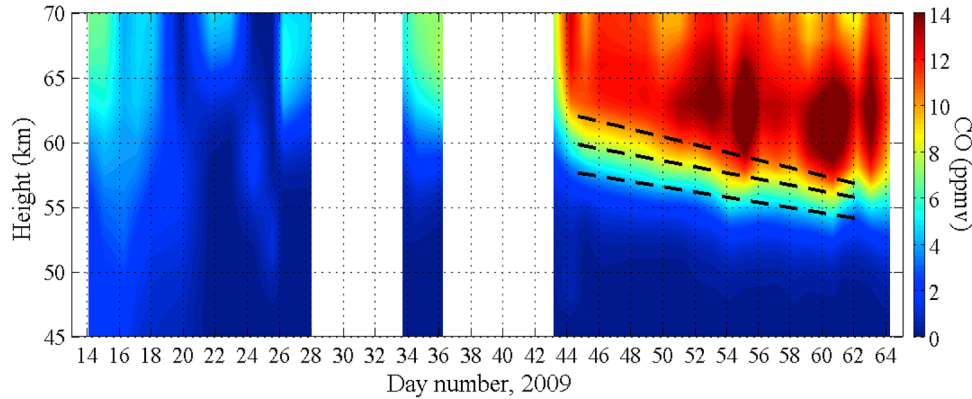


Figure 9. Contour plot of CO mr between 45 and 70 km in the period 14 January to 5 March 2009 (days 14–64). Linear fits to CO mr levels of 5, 8 and 11 ppmv altitude versus time are also shown (dashed lines).

to 0.30 ± 0.05 km/day, gradually increasing with increasing starting altitude. We compared these estimates with approximate values that can be extrapolated from Figures 2 and 4 of *Orsolini et al.* [2010]. Using their 4 and 5 ppmv Odin/submillimeter radiometer H₂O mr contour lines (located, at the beginning of February, approximately at 0.08 hPa or 62 km and 0.13 hPa or 59 km), we estimate a descent rate of 0.3 km/day (following the 4 ppmv contour) and 0.2 km/day (following the 5 ppmv contour). Although the agreement with our descent rates is very good, it should be emphasized that the estimates obtained from the work of *Orsolini et al.* [2010] are based on data averaged over the whole polar region northward of 70°N.

4. Summary

[29] Ground-based measurements of middle atmospheric profiles of temperature, O₃, CO, and N₂O mr were carried out from Thule, Greenland, during winter 2008–2009. These measurements add further information to previous analyses aimed at studying the evolution of the 2009 winter stratosphere and tracking the exceptional SSW that occurred during the second half of January. The main findings of this analysis are as follows.

[30] 1. In the first part of January the polar vortex was stable and cold. PSCs were detected between 17 and 22 km on 18–19 January (not shown).

[31] 2. At Thule the SSW event was initially detected at ~ 2000 K on 19 January by a rapid decrease in CO mr. The first evidence of a temperature increase was observed at about 50 km on 22 January, when lidar measurements were first able to reach this altitude. The warming progressed downward, reaching about 15 km altitude on 29 January. The maximum physical temperature, 289 K, was observed at layers between 1300 and 1500 K on 22 January. In late January the temperature profile became near isothermal, particularly in the altitude layer between 15 and 45 km.

[32] 3. Backward trajectories at the various altitudes studied indicate that air masses approaching the polar region during the warming peak were subjected to a rapid compression and an intense adiabatic warming. This is estimated to maximize with $\Delta T \sim 50$ K at $\sim 1000 \div 1300$ K.

[33] 4. The passage of the vortex edge over Thule associated with the vortex breakup was marked by a sudden increase in N₂O and decrease in CO mr's measured by the GBMS below and above 1000 K, respectively. PV, N₂O, and CO are in good agreement in identifying the vortex breakup. The vortex re-formed rapidly and strongly above 1000 K at the beginning of February, but not in the lower stratosphere. Rapid changes in N₂O, O₃, and CO are associated with the advection of air masses of different origins, in some cases not detected by PV analyses. Maxima in N₂O mr in late January and mid-February are associated with rapid transport of extratropics air masses.

[34] 5. Mesospheric CO measurements inside the re-formed vortex indicate descent rates between 0.30 ± 0.05 and 0.20 ± 0.05 km/day for starting altitudes between 62 and 58 km, respectively, from mid-February to early March.

[35] **Acknowledgments.** This work was supported by the project PRIN 2007 (Dirigibile Italia), funded by the Italian Ministry for University and Research, and by the Italian Antarctic Program. We would like to thank the NSF and Susan Zager of CH2M HILL Polar Services for logistic support and NASA GSFC for the trajectory Automailer system. We are grateful to C. Cesaroni for his assistance during the field campaign. Contributions by S. E. Ascanius, M. Cacciani, G. Casasanta, V. Ciardini, T. Di Iorio, and C. Tirelli are gratefully acknowledged. We thank Gloria Manney and the MLS team for making available the AURA/MLS data plots displayed in Figure 6. Helpful comments and suggestions from three anonymous reviewers are also acknowledged.

References

- Barnett, J. J., and M. Corney (1985), Middle atmosphere reference model derived from satellite data, *Handbk. MAP*, 16, 47–137.
- Charlton, A. J., and L. Polvani (2007), A new look at stratospheric sudden warmings. Part I: Climatology and modeling benchmarks, *J. Clim.*, 20, 449–469.
- de Zafra, R. L. (1995), The ground-based measurements of stratospheric trace gases using quantitative millimeter wave emission spectroscopy, in *Diagnostic Tools in Atmospheric Physics, Proceedings of the International School of Physics “Enrico Fermi,”* vol. 124, pp. 23–54, Soc. It. di Fis., Bologna, Italy.
- de Zafra, R. L., and G. Muscari (2004), CO as an important high-altitude tracer of dynamics in the polar stratosphere and mesosphere, *J. Geophys. Res.*, 109, D06105, doi:10.1029/2003JD004099.
- di Sarra, A., M. Cacciani, G. Fiocco, D. Fuà, and T. S. Jørgensen (2002), Lidar observations of polar stratospheric clouds over northern Greenland in the period 1990–1997, *J. Geophys. Res.*, 107(D12), 4152, doi:10.1029/2001JD001074.

- Fiorucci, I., et al. (2008), Measurements of low amounts of precipitable water vapor by millimeter wave spectroscopy: An intercomparison with radiosonde, Raman lidar, and Fourier transform infrared data, *J. Geophys. Res.*, *113*, D14314, doi:10.1029/2008JD009831.
- Keckhut, P., et al. (2004), Review of ozone and temperature lidar validations performed within the framework of the Network for the Detection of Stratospheric Change, *J. Environ. Monit.*, *6*, 721–733.
- Harada, Y., A. Gotoh, H. Hasegawa, and N. Fujikawa (2010), A major stratospheric sudden warming event in January 2009, *J. Atmos. Sci.*, *67*, 2052–2069.
- Labitzke, K., and M. Kunze (2009), On the remarkable Arctic winter 2008/2009, *J. Geophys. Res.*, *114*, D00102, doi:10.1029/2009JD012273.
- Labitzke, K., and H. van Loon (1988), Associations between the 11-year solar cycle, the QBO and the atmosphere. Part I: The troposphere and the stratosphere in the Northern Hemisphere winter, *J. Atmos. Terr. Phys.*, *50*, 197–206.
- Manney, G. L., K. Krüger, J. L. Sabutis, S. A. Sena, and S. Pawson (2005), The remarkable 2003–2004 winter and other recent warm winters in Arctic stratosphere since 1990s, *J. Geophys. Res.*, *110*, D04107, doi:10.1029/2004JD005367.
- Manney, G. L., et al. (2008), The evolution of the stratopause during the 2006 major warming: Satellite data and assimilated meteorological analyses, *J. Geophys. Res.*, *113*, D11115, doi:10.1029/2007JD009097.
- Manney, G. L., et al. (2009), Aura Microwave Limb Sounder observations of dynamics and transport during the record-breaking 2009 Arctic stratospheric major warming, *Geophys. Res. Lett.*, *36*, L12815, doi:10.1029/2009GL038586.
- Marengo, F., et al. (1997), Thermal structure of the winter middle atmosphere observed by lidar at Thule, Greenland, during 1993–1994, *J. Atmos. Sol. Terr. Phys.*, *59*(2), 151–158.
- Matthewman, N. J., J. G. Esler, A. J. Charlton-Perez, and L. M. Polvani (2009), A new look at stratospheric sudden warmings. Part III: Polar vortex evolution and vertical structure, *J. Clim.*, *22*, 1566–1585.
- Muscati, G., A. G. di Sarra, R. L. de Zafra, F. Lucci, F. Baordo, F. Angelini, and G. Fiocco (2007), Middle atmospheric O₃, CO₂, N₂O, HNO₃, and temperature profiles during the Arctic winter 2001–2002, *J. Geophys. Res.*, *112*, D14304, doi:10.1029/2006JD007849.
- Orsolini, Y. J., J. Urban, D. Murtagh, S. Lossow, and V. Lympasuvan (2010), Descent from the polar mesosphere and anomalously high stratopause observed in 8 years of water vapor and temperature satellite observations by the Odin submillimeter radiometer, *J. Geophys. Res.*, *115*, D12305, doi:10.1029/2009JD013501.
- Schoeberl, M. R. (1978), Stratospheric warmings: Observations and theory, *Rev. Geophys.*, *16*(4), 521–538.
- Schoeberl, M. R., and L. C. Sparling (1994), Trajectory modelling, in *Diagnostic Tools in Atmospheric Physics, Proceedings, SIF Course CXVI*, edited by G. Fiocco and G. Visconti, North-Holland, Amsterdam.
- van Loon, H., and K. Labitzke (1987), The Southern Oscillation. Part V: The anomalies in the lower stratosphere of the Northern Hemisphere in winter and a comparison with the Quasi-Biennial Oscillation, *Mon. Weather Rev.*, *115*, 357–369.
-
- R. L. de Zafra, Department of Physics and Astronomy, State University of New York at Stony Brook, Stony Brook, NY 11794, USA.
- C. Di Biagio and A. di Sarra, ENEA/UTMEA-TER, via Anguillarese 301, Santa Maria di Galeria, I-00123 Rome, Italy. (claudia.dibbiagio@enea.it)
- P. Eriksen, Danish Meteorological Institute, Lyngbyvej 100, DK-2100, Copenhagen, Denmark.
- G. Fiocco and D. Fuà, Department of Physics, University of Rome “Sapienza,” Viale dell’Università 30, I-00185 Rome, Italy.
- G. Muscati and I. Fiorucci, Istituto Nazionale di Geofisica e Vulcanologia, Via di Vigna Murata 605, I-00143 Rome, Italy.